Quasi-elastic Neutron Scattering Reveals Ligand-Induced Protein Dynamics of a G-Protein-Coupled Receptor

Utsab R. Shrestha,[†,¶] Suchithranga M. D. C. Perera,[‡,¶] Debsindhu Bhowmik,[†,§] Udeep Chawla,[‡] Eugene Mamontov,[∥] Michael F. Brown,[‡,⊥] and Xiang-Qiang Chu[*,†]

[†]Department of Physics and Astronomy, Wayne State University, Detroit, Michigan 48201, United States
[‡]Department of Chemistry and Biochemistry, University of Arizona, Tucson, Arizona 85721, United States
[§]Computational Science and Engineering Division, Oak Ridge National Laboratory, Oak Ridge, Tennessee 37831, United States
[∥]Chemical and Engineering Materials Division, Oak Ridge National Laboratory, Oak Ridge, Tennessee 37831, United States
[⊥]Department of Physics, University of Arizona, Tucson, Arizona 85721, United States

S Supporting Information

ABSTRACT: Light activation of the visual G-protein-coupled receptor (GPCR) rhodopsin leads to significant structural fluctuations of the protein embedded within the membrane yielding the activation of cognate G-protein (transducin), which initiates biological signaling. Here, we report a quasi-elastic neutron scattering study of the activation of rhodopsin as a GPCR prototype. Our results reveal a broadly distributed relaxation of hydrogen atom dynamics of rhodopsin on a picosecond–nanosecond time scale, crucial for protein function, as only observed for globular proteins previously. Interestingly, the results suggest significant differences in the intrinsic protein dynamics of the dark-state rhodopsin versus the ligand-free apoprotein, opsin. These differences can be attributed to the influence of the covalently bound retinal ligand. Furthermore, an idea of the generic free-energy landscape is used to explain the GPCR dynamics of ligand-binding and ligand-free protein conformations, which can be further applied to other GPCR systems.
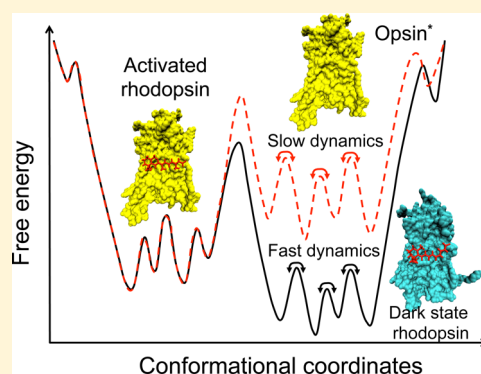
Protein dynamics are the key to understanding the biological activities[1,2] of pharmacologically important biological systems such as G-protein-coupled receptors (GPCRs).[3–6] Conformational fluctuations of the protein upon extracellular stimulation lead to activation of GPCRs in a cellular membrane lipid environment. X-ray crystallographic experiments[7] and recent time-resolved wide-angle X-ray scattering (WAXS) studies[8] conducted on the prototypical visual GPCR rhodopsin have revealed valuable information about the conformational changes that occur during activation. However, thus far, little information is available regarding how the internal dynamics evolve during GPCR function.[9] In this Letter, we use the quasi-elastic neutron scattering (QENS) technique to study the changes in GPCR mobility upon activation with rhodopsin as a prototype.

Rhodopsin is a class A GPCR responsible for scotopic vision in vertebrates. It is the canonical prototype of the *Rhodopsin* family of GPCRs.[5] The chromophore 11-*cis*-retinal locks the rhodopsin in the inactive dark state,[10] and it acts as an inverse-agonist by preventing interaction with its cognate G-protein (transducin). Upon photon absorption, the 11-*cis*-retinal isomerizes to all-*trans*, yielding rearrangement of the protein conformation by two protonation switches.[11,12] The photoisomerization of retinal occurs within 200 fs, causing rhodopsin to undergo a series of multiscale transitions.[13,14] Currently, X-ray crystal structures are

available for rhodopsin in the dark state,[15,16] as well as several freeze-trapped photointermediates,[7,17] including the ligand-free opsin apoprotein. Both solid-state NMR methods[9,13] and site-directed spin labeling (SDSL) have been extensively applied to study rhodopsin.[18] Here we compared the protein dynamics of the dark-state rhodopsin to those of ligand-free opsin produced from active metarhodopsin-II in the visual signaling mechanism. Both elastic and quasi-elastic neutron scattering were utilized[19,20] with the aim of studying the functional protein dynamics that lead to transducin activation.[13]

Intrinsic fluctuations of protein structures are due to a large number of conformational substates (CSs) represented by a hierarchical (rough) energy landscape (EL),[21,22] as first discussed for globular proteins by Frauenfelder et al.[2] The protein dynamics encompass a broad range of time scales, ranging from local motions (ps–ns) to collective domain motions (ns–μs).[1,22,23] In analogy with glass-forming liquids, the short-time dynamics (β-relaxation) include small-amplitude local motions (e.g., side chains and methyl group rotations), whereas the long-time dynamics (α-relaxation) are due to collective protein motions of larger amplitude. To date, mainly

globular proteins such as myoglobin[2] and lysozyme[24] have been studied with this approach. Experimentally, we prove that the EL concept is also valid for membrane proteins such as GPCRs and apply it to explain the changes in the ligand binding of GPCR rhodopsin upon photoactivation. Notably, QENS can be used to study the relaxation dynamics of hydrogen atoms due to vibrations, relaxations, and rotations within the protein molecule.[19,25] Advances in the QENS technique were exploited to probe the effect of the retinal cofactor on the dynamics of rhodopsin in the β-relaxation time range (ps−ns) crucial for its activation. Light-induced isomerization of the 11-cis-retinal cofactor and the subsequent release of the chromophore unlock the intrinsic protein dynamics in the ligand-free opsin state, followed by interaction with the heterotrimeric G-protein (transducin). Our QENS experiments probed the hydrogen atom dynamics in the β-relaxation range for the dark-state rhodopsin and ligand-free opsin. We discovered that the local relaxation dynamics in the opsin apoprotein are slower compared to those in the dark-state rhodopsin, which corresponds to the open conformation of opsin and thus more degrees of freedom for protein movement due to the removal of retinal cofactor.

In our neutron scattering experiments, we use D_2O-hydrated dark-state rhodopsin and ligand-free apoprotein opsin with hydration level $h \approx 0.27$ (i.e., 0.27 gram of D_2O per gram of protein). A detergent 3-[(3-cholamidopropyl)dimethyl-ammonio]-1 propanesulfonate (CHAPS) was chosen to have a minimum detergent/protein ratio, as described in the Supporting Information (SI). First, we employed elastic incoherent neutron scattering (EINS)[26,27] to determine whether the dissociation of the retinal ligand from rhodopsin affects the protein flexibility, as shown in Figure 1. The mean-squared
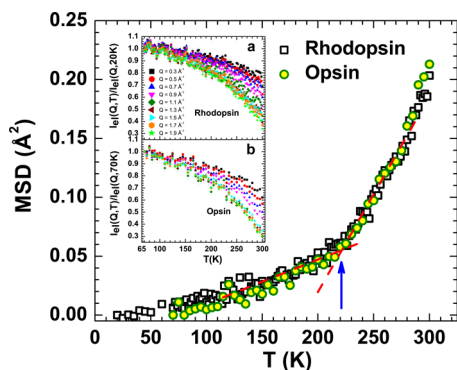

Figure 1. MSDs of hydrogen atoms in rhodopsin and its ligand-free apoprotein opsin are nearly identical and show a dynamical transition at $T_D \approx 220$ K. MSDs of hydrogen atoms in dark-state rhodopsin (open black squares) and ligand-free opsin (open green circles) are shown as functions of temperature. The inset shows the EINS intensities for dark-state rhodopsin (a) and opsin (b).

displacement (MSD), denoted by $\langle x^2(T) \rangle$, is traditionally used as the index of "softness" or flexibility of globular proteins.[28] It can be calculated from the EINS intensities by applying a Gaussian approximation to the Lamb−Mössbauer factor, which is valid for small Q values,[29] $S_H(Q,T,\omega=0) = \exp(-Q^2\langle x^2(T)\rangle)$. Here, $S_H(Q,T,\omega=0)$ is calculated from the ratio of the temperature-dependent elastic intensity, $I_{elastic}(Q,T,\omega = 0)$, and the elastic intensity at the lowest measured temperature, $I_{elastic}(Q,T\approx0,\omega=0)$. The slope of the logarithm of $S_H(Q,T,\omega=0)$ versus Q^2 yields the MSD $\langle x^2(T) \rangle$ (see the SI

for details). In combination, EINS and QENS allow one to investigate both equilibrium and dynamical properties.

The calculated MSDs are plotted as a function of temperature in Figure 1 for both dark-state rhodopsin and the ligand-free apoprotein, opsin. According to the plot, for rhodopsin versus opsin, there is no major difference in hydrogen atom MSDs of the samples within the measured temperature range. Notably, there is a sudden increase in the slope of the MSDs above the so-called dynamical transition temperature of $T_D \approx 220$ K,[30] indicating an onset of rapid thermal fluctuations among the substates of both rhodopsin and opsin. This dynamical transition in hydrated proteins reveals the change in the motion of protein functional groups from harmonic to anharmonic behavior. Above T_D, sufficient energy is acquired for atoms to move anharmoni-cally among the various substates or potential wells. At this point, we can conclude that above $T_D \approx 220$ K the membrane protein rhodopsin attains the conformational flexibility required to perform its biological function, which is cofactor-independent. In the following sections, we describe how the cofactor-dependent hydrogen atom dynamics are studied using the QENS technique.

Next, we conducted QENS measurements on both samples at temperatures ranging from T = 220 to 300 K, with momentum transfer Q ranging from 0.3 to 1.9 Å^{-1}. The measured QENS spectra for both rhodopsin and opsin are illustrated in Figure 2a,b, respectively, at nine different temperatures and $Q = 1.1$ Å^{-1}. The measured QENS intensity, that is, the self-dynamic incoherent scattering structure factor $S_m(Q,\omega)$, shows an increase in quasi-elastic broadening with temperature, indicating faster ps−ns diffusive motions of the hydrogen atoms within the protein molecules. In QENS, the elastic component (central peak) originates from the immobile atoms within the experimental energy (or time) window.[31] The quasi-elastic components (broadenings from the elastic central peak or the resolution function) are due to spatial motion of the mobile atoms (see the SI for details).

The analysis of $S_m(Q,\omega)$ using a classical approach was implemented to scrupulously decouple the motions of the detergent (CHAPS) and the protein.[32] Figure 2c,d demonstrates the analysis of the measured $S_m(Q,\omega)$ as a superposition of a Dirac delta function, two Lorentzians (L_1 and L_2), and a linear background convoluted with the resolution function, within the energy-transfer range ±110 μeV for rhodopsin and opsin, respectively. The full width at half-maximum (FWHM, 2Γ) of the Lorentzians provides information about the motions of hydrogen atoms within the samples. According to the analysis as shown in Figure 2c,d, the FWHM of $L_1(2\Gamma_1)$ is much broader than that of $L_2(2\Gamma_2)$ and is Q-independent (details are shown in Figures S1 and S2 in the SI), with the values very close to the FWHM values extracted from the analysis of the QENS data of the pure CHAPS sample. By contrast, the FWHM of $L_2(2\Gamma_2)$ is much narrower and Q-dependent compared to that of $L_1(2\Gamma_1)$. Thus, we can confidently attribute the faster CHAPS dynamics to L_1 and the slower protein dynamics to the L_2 component. Using this classical approach, we can then readily separate the dynamics of rhodopsin and the detergent CHAPS, which has been successfully applied in the analysis of previous QENS data.[19,32]

The energy domain analysis is summarized in Figure 2e, where we plot the relaxation time (τ) for diffusive motion of the hydrogen atoms of rhodopsin and opsin versus Q at temperatures between T = 260 and 300 K. The relaxation time (τ) was calculated using the relation $\tau = \hbar/2\Gamma_2$, corresponding to the diffusive motion due to solvent-slaved[2] or solvent-independent processes[33] at measured length scales. Our results show that at
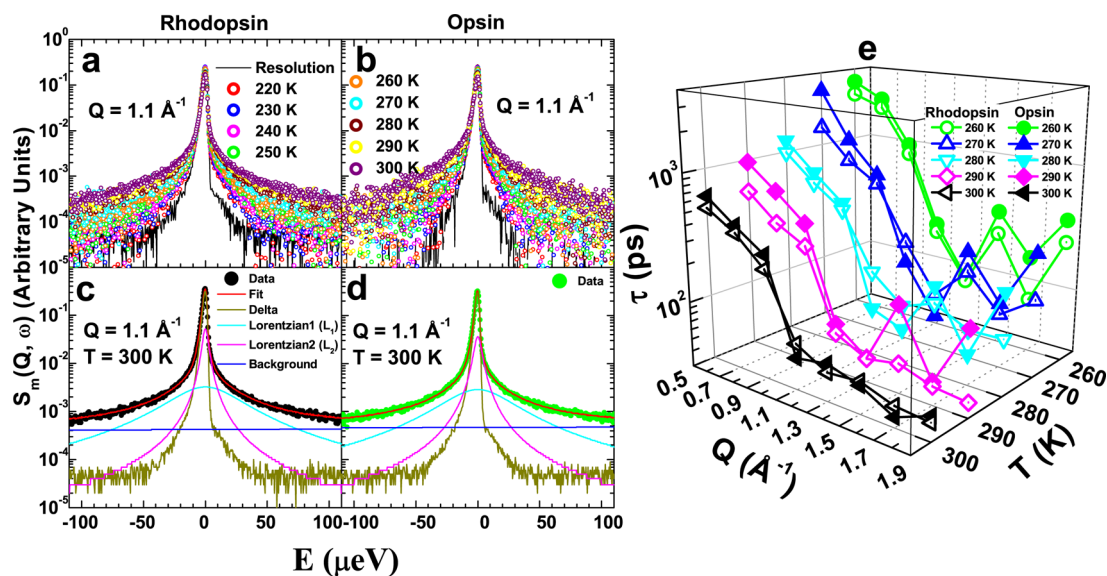
Figure 2. Ligand-free opsin apoprotein shows slower hydrogen atom dynamics compared to the dark-state rhodopsin. (Left) QENS spectra for dark-state rhodopsin and ligand-free opsin samples. (a,b) Normalized dynamic incoherent scattering function, $S_m(Q,\omega)$ from two samples at $Q = 1.1$ Å^{-1} from 220 to 300 K along with the resolution function. (c,d) Analysis of the QENS spectra at $Q = 1.1$ Å^{-1} and $T = 300$ K, showing the elastic scattering component (delta function), quasi-elastic scattering components (two Lorentzians indicated by cyan and magenta lines), background (blue line), and the fitted curves (red line). (e) Comparison of the relaxation time (τ) of dark-state rhodopsin and ligand-free opsin as a function of Q for $T = 260-300$ K in 10 K steps.

low Q values the diffusive motion of the hydrogen atoms is slower in opsin (reflected in larger τ values) compared to that of rhodopsin across all measured temperatures, as shown in Figure 2e. This manifests two types of motional dynamics: small Q, long-range with very slow "true" diffusion, and midrange Q, protein-local dynamics at about 1.6 Å^{-1}. In the Q range from 0.5 to 0.9 Å^{-1}, the relaxation time of both states decreases with Q due to diffusive motion over a length scale of >7 Å. However, in the larger Q range from 1.1 to 1.9 Å^{-1}, the relaxation time reaches its minimum value at around 1.3–1.8 Å^{-1} and is barely Q-dependent, indicating that the motion in protein is localized on length scales < 6 Å. The analysis in the energy domain gives us an initial indication that the diffusive motion of the hydrogen atoms is slower in opsin as compared to that in rhodopsin, prompting us to extend the analysis to the time domain, as we describe below.

To further investigate the differences in hydrogen atom motions in dark-state rhodopsin versus that in the ligand-free apoprotein opsin, we evaluated the relaxation dynamics in the real-time domain. The inverse Fourier transform of the QENS data measured in the energy domain yields the intermediate scattering function (ISF), denoted by $I(Q,t)$ of the measured spectra in the time domain, as described in the SI. In QENS measurements, the ISF represents the single-particle correlation function of hydrogen atoms. It is the essential function to describe the relaxation dynamics and can be directly connected to the theoretical calculations[34,35] and molecular dynamics (MD) simulations.[36,37] In our analysis, the contribution of the detergent intensity was subtracted before Fourier transformation, according to our energy domain analysis[38] (see the SI for details). The ISF, denoted by $I(Q,t)$ of hydrogen atoms in rhodopsin and opsin, is plotted near the physiological temperature $T = 300$ K, as shown in Figure 3 at a series of Q values. Further analysis at a series of different temperatures $T = 260, 280,$ and 300 K is shown in Figure S3.
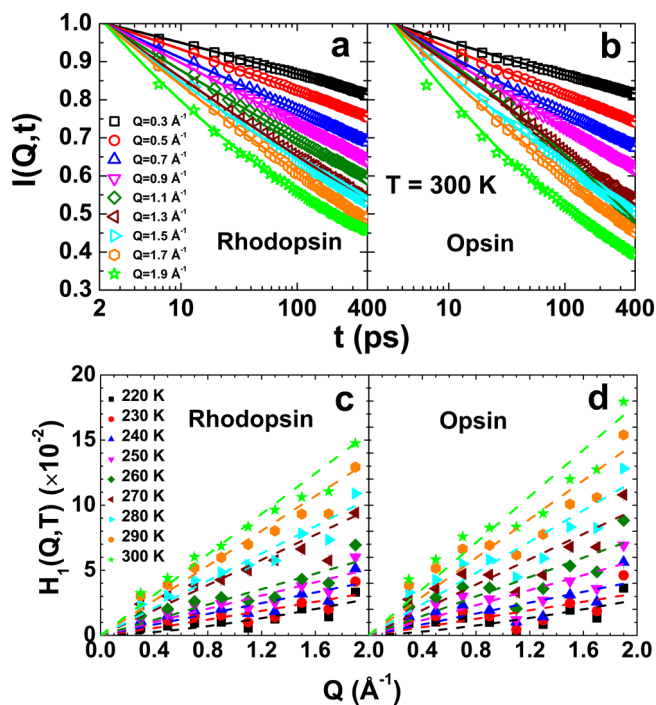

Figure 3. Mode-coupling theory (MCT) analysis of QENS data in the time domain. (a,b) ISF $I(Q,t)$ of dark-state rhodopsin and opsin at $T = 300$ K at Q values from 0.3 to 1.9 Å^{-1} with 0.2 Å^{-1} steps. Solid lines are fits to the ISF with a logarithmic decay model for the β-relaxation region of protein dynamics at various Q values. (c,d) First-order logarithmic decay parameter $H_1(Q,T)$ as a function of Q for dark-state rhodopsin and opsin, respectively.

From theoretical predictions, the protein dynamics at different time scales can be approximately divided into three groups:[22,39] (i) a short-lived Gaussian-like ballistic region due to vibrations; (ii) fast dynamics in the β-relaxation region (ps–ns) governed by
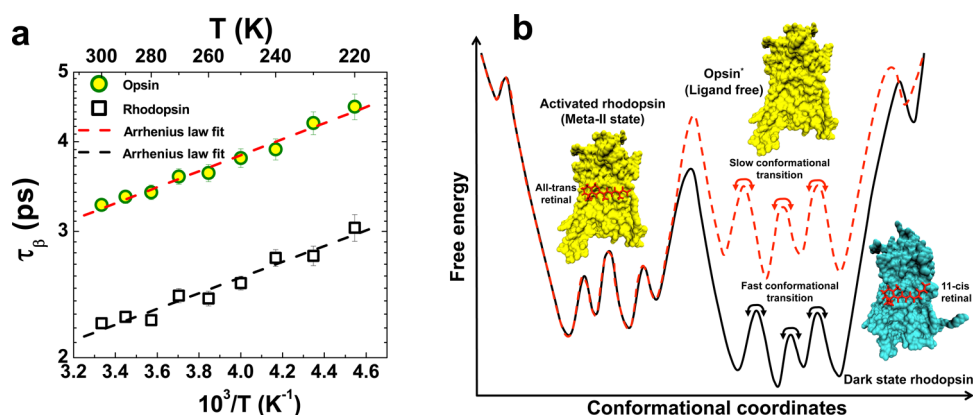
Figure 4. Free-EL model for the rhodopsin activation process. (a) Arrhenius plot of the characteristic β-relaxation time (τ_β) as a function of inverse temperature for dark-state rhodopsin and opsin. Yellow-filled green circles represent τ_β of opsin, open black squares denote dark-state rhodopsin, and dashed red and black lines represent the τ_β values fitted with the Arrhenius law. The activation energies (E_β) of the atomic fluctuations for dark-state rhodopsin and ligand-free opsin apoprotein are 2.14 ± 0.17 and 2.18 ± 0.11 kJ/mol, respectively. (b) Schematic free-energy model representing the rhodopsin activation process. The black curve displays the free energy of ligand-binding rhodopsin, as a function of arbitrary conformational coordinates. The red curve represents the free energy of ligand-free opsin.

a logarithmic decay; followed by (iii) slow dynamics[40,41] in the α-relaxation region (μs−ms) given by a stretched-exponential decay. The correlation between dynamics and biological activity has been demonstrated on the μs−ms time scale, but fluctuations at the atomic level are much faster than this.[21,42,43] Our experimental results correspond to the β-relaxation region within the time window of picoseconds−nanoseconds. Upon increasing temperature, the protein local dynamics become faster in both rhodopsin and opsin. Furthermore, the Q dependence of the ISFs indicates that the relaxation process varies within the different length scales in the sample (from Å up to nm). Notably, rhodopsin and opsin (both membrane proteins) demonstrate the characteristic broadly distributed relaxation rates of the ISF in the β-relaxation regime, previously observed only in aqueous soluble globular proteins.[24,37,44]

Having observed the broadly distributed rates in the ISFs of both rhodopsin and opsin, we next applied mode-coupling theory (MCT) to fathom the differences in β-relaxation (1−400 ps) dynamics for opsin versus rhodopsin. The MCT was originally developed to describe the complex dynamics in glass-forming liquids,[45−47] and has also been successfully used in describing the β-relaxation dynamics of globular proteins and other biopolymers.[24,37,44,48] The ISFs can be fitted with an asymptotic expression derived from the MCT for systems close to higher-order singularity as[49]

$$I(Q, t) = f(Q, T) - H_1(Q, T) \ln[t/\tau_\beta(T)]$$
$$+ H_2(Q, T) \ln^2[t/\tau_\beta(T)] \qquad (1)$$

Here $\tau_\beta(T)$ is the characteristic β-relaxation time, which corresponds to the characteristic of fast motion, such as methyl group rotations in protein, and $f(Q,T) = \exp[-A(T)Q^2]$ is related to the Debye−Waller factor for the small Q values. The quantities $H_1(Q,T)$ and $H_2(Q,T)$ are the Q- and T-dependent first- and second-order logarithmic decay parameters, respectively, which depend on the distance of the state point from the singularity (also known as separation parameters)[49] and are measures of broadly distributed rates in relaxation processes. The fitting parameter $H_1(Q,T)$ is shown in Figure 3c,d for rhodopsin and opsin, respectively. It is qualitatively understood as the slope of the decay, or the power of the decay, and can be expressed as a power law in Q as given by $H_1(Q,T) = B_1(T)Q^\beta$, where the

exponent can take the values $\beta \approx 1-2$ and $B_1(T)$ is a temperature-dependent parameter, as shown in Figure S4.

The active opsin resembles the more open metarhodopsin-II active structure due to tilting of transmembrane helices H5 and H6 away from the H1−H4 core.[15] Thus, one could expect the slower dynamics in opsin because of its open conformation[50] due to the isomerization of 11-*cis*-retinal upon activation followed by the removal of any retinal cofactor. The characteristic β-relaxation time (τ_β) values from fitting the ISF by eq 1 are summarized in Figure 4a. Notably, we observed longer β-relaxation times (τ_β) in opsin for the temperatures ranging from 220 to 300 K, which suggests that the ligand-free opsin has an open conformation compared to that of dark-state rhodopsin, whose conformation is locked by 11-*cis*-retinal. In the temperature range of 220−300 K, the τ_β values of both rhodopsin and opsin follow an Arrhenius behavior, $\tau_\beta = \tau_0 \exp(E_a/RT)$, where R is the gas constant and E_a is the average activation energy that can be attributed to the β-relaxation process due to protein motions such as methyl group rotations. The E_a values calculated for both dark-state rhodopsin (2.14 ± 0.17 kJ/mol) and ligand-free opsin (2.18 ± 0.11 kJ/mol) are almost identical.

One should recognize that protein flexibility and ligand binding are coupled to each other, which is conventionally described by different biophysical models.[51] In Figure 4b, we plot a schematic free-EL model representing the rhodopsin activation process, where vertical and horizontal axes represent the free-energy and conformational coordinates, respectively. Conformational coordinates refer to the large number of slightly different conformations (known as CSs) of the protein around its average structure with small barrier heights, which forms the multi-dimensional free-EL.[1] The black curve in Figure 4b models the free energy of ligand-binding rhodopsin or dark-state rhodopsin, and the red curve represents the free energy of ligand-free opsin. The free-energy differences between the different states contain many contributions, including direct protein−ligand interactions, hydrophobic association, and the conformational and vibrational entropy of rhodopsin and retinal. Such hierarchical ELs are reflected by the small fluctuations in the curves, as shown in Figure 4b. This schematic picture explains the mechanisms of rhodopsin conformational changes and protein dynamics during photoactivation. Among the features of the complex system is highly nonexponential relaxation,[39,47] which describes the EL

due to the many CSs with similar energies. The different basins of the EL give us a framework for understanding the conformational changes during a reaction, such as GPCR activation of the cognate G-protein. Because the fluctuations are thermally driven, temperature plays a major role.[30] At sufficiently low temperature, the individual protein molecules are trapped in various potential wells, where they undergo harmonic vibrations due to the CSs, which are separated by smaller energy barriers between them.[19]

According to our results, the ligand-free opsin has a larger characteristic β-relaxation time due to its open conformation compared to that of the dark-state rhodopsin, where the 11-*cis*-retinal locks the protein conformation. Such dynamic behavior suggests that 11-*cis*-retinal confines the protein conformation in the lowest possible energy or the ground state, as shown in the protein free-EL picture (see Figure 4b). Upon photoactivation, the 11-*cis*-retinal isomerizes to all-*trans* and the subsequent removal of retinal from the ligand-binding pocket yields an open conformation, as suggested by the slower relaxation dynamics. Such protein conformations are the excited states with higher energy barriers, as shown in Figure 4b. The slower dynamics of opsin may be crucial for the catalytic activation of the cognate G-protein (transducin), which is due to the lack of stabilizing interactions between the retinal chromophore and the secondary structures involving the receptor-binding pocket. The stabilizing forces in opsin are weaker compared to those for the dark-state rhodopsin, which is consistent with an ensemble-activation mechanism of the visual GPCR rhodopsin.[52] Furthermore, the influences of both temperature and hydration[19,23,53,54] then allow one to further address the EL in terms of a hierarchical organization.[2] As the all-*trans*-retinal binds to the rhodopsin, the water molecules in the solvent shell surrounding the hydrophobic moieties of the ligand and binding site will be released to the bulk solvent and gain entropy; thereby, the free energy of the dark-state rhodopsin is lower than that of opsin.[51] In addition, when binding to small but solvent-accessible hydrophobic cavities of rhodopsin, the disordered water molecules have a density much lower than the bulk water density, which therefore will increase the solvent free energy. Increased hydration upon light activation is fully consistent with recent MD simulation results.[55]

In summary, QENS data from the dark-state rhodopsin and the ligand-free apoprotein, opsin, were analyzed in the energy domain by a classical approach to decouple the detergent and protein dynamics and in the time domain by MCT, as originally formulated to describe the complex dynamics in glass-forming liquids.[47] With this combined approach, we show a larger and detailed picture of the ligand-induced GPCR dynamics. Significantly, MCT analysis of a membrane protein, rhodopsin, demonstrates a broadly distributed relaxation similar to the one previously observed for globular proteins.[24] The light causes isomerization of 11-*cis*-retinal, which unlocks the intrinsic dynamics of the dark-state rhodopsin that are pivotal for the activation mechanism. Both energy and time domain analysis of the QENS data show that the dynamics of the ligand-free apoprotein, opsin (yielded after the photoactivation), are significantly slower compared to those of dark-state rhodopsin, which is locked by 11-*cis*-retinal, suggesting the open conformation and thus more degrees of freedom for protein movement in opsin, crucial for the activation of cognate G-protein (transducin).[10] These results confirm that the retinal cofactor influences the dynamics in the activation mechanism of a canonical prototype for *Rhodopsin* (Family A) GPCRs. Such a change in protein dynamics due to the removal of retinal in opsin

is necessary for the interaction between the rhodopsin GPCR and its cognate G-protein, yielding the catalytic activation of transducin. Our results are consistent with the regulation of protein structural dynamics by the retinal cofactor of rhodopsin. Furthermore, a schematic free-EL picture explains our findings, which support protein dynamics changes in the absence of the retinal cofactor due to the open conformation upon removal of retinal. These findings pave the road to study the crucial dynamic behavior of other biologically important membrane proteins in the GPCR superfamily. An important question remaining for future research is whether active metarhodopsin-II yields results consistent with greater flexibility of the protein structure as compared to the apoprotein opsin due to the presence of all-*trans*-retinal.

■ ASSOCIATED CONTENT

Ⓢ Supporting Information

The Supporting Information is available free of charge on the ACS Publications website at DOI: 10.1021/acs.jpclett.6b01632.

Sample preparation, experimental methods and details of the data analysis (PDF)

■ AUTHOR INFORMATION

Corresponding Author
*E-mail: chux@wayne.edu. Phone: 313-577-8962.

Author Contributions
¶U.R.S. and S.M.D.C.P. contributed equally.

Notes
The authors declare no competing financial interest.

■ ACKNOWLEDGMENTS

■ REFERENCES

(1) Henzler-Wildman, K.; Kern, D. Dynamic Personalities of Proteins. *Nature* 2007, *450*, 964−972.

(2) Frauenfelder, H.; Chen, G.; Berendzen, J.; Fenimore, P. W.; Jansson, H.; McMahon, B. H.; Stroe, I. R.; Swenson, J.; Young, R. D. A Unified Model of Protein Dynamics. *Proc. Natl. Acad. Sci. U. S. A.* 2009, *106*, 5129−5134.

(3) Chung, K. Y.; Rasmussen, S. G.; Liu, T.; Li, S.; DeVree, B. T.; Chae, P. S.; Calinski, D.; Kobilka, B. K.; Woods, V. L., Jr.; Sunahara, R. K. Conformational Changes in the G Protein Gs Induced by the Beta2 Adrenergic Receptor. *Nature* 2011, *477*, 611−615.

(4) Venkatakrishnan, A. J.; Deupi, X.; Lebon, G.; Tate, C. G.; Schertler, G. F.; Babu, M. M. Molecular Signatures of G-Protein-Coupled Receptors. *Nature* 2013, *494*, 185.

(5) Lagerström, M. C.; Schioth, H. B. Structural Diversity of G Protein-Coupled Receptors and Significance for Drug Discovery. *Nat. Rev. Drug Discovery* 2008, *7*, 542.

(6) Rosenbaum, D. M.; Rasmussen, S. G. F.; Kobilka, B. K. The Structure and Function of G-Protein-Coupled Receptors. *Nature* **2009**, *459*, 356−363.

(7) Choe, H.-W.; Kim, Y. J.; Park, J. H.; Morizumi, T.; Pai, E. F.; Krauß, N.; Hofmann, K. P.; Scheerer, P.; Ernst, O. P. Crystal Structure of Metarhodopsin II. *Nature* **2011**, *471*, 651−655.

(8) Malmerberg, E.; M. Bovee-Geurts, P. H.; Katona, G.; Deupi, X.; Arnlund, D.; Wickstrand, C.; Johansson, L. C.; Westenhoff, S.; Nazarenko, E.; X. Schertler, G. F.; Menzel, A.; de Grip, W. J.; Neutze, R. Conformational Activation of Visual Rhodopsin in Native Disc Membranes. *Sci. Signaling* **2015**, *8*, ra26−ra26.

(9) Struts, A. V.; Salgado, G. F.; Brown, M. F. Solid-State 2H NMR Relaxation Illuminates Functional Dynamics of Retinal Cofactor in Membrane Activation of Rhodopsin. *Proc. Natl. Acad. Sci. U. S. A.* **2011**, *108*, 8263−8268.

(10) Kawamura, S.; Gerstung, M.; Colozo, A. T.; Helenius, J.; Maeda, A.; Beerenwinkel, N.; Park, P. S.; Muller, D. J. Kinetic, Energetic, and Mechanical Differences between Dark-State Rhodopsin and Opsin. *Structure* **2013**, *21*, 426−437.

(11) Mahalingam, M.; Martinez-Mayorga, K.; Brown, M. F.; Vogel, R. Two Protonation Switches Control Rhodopsin Activation in Membranes. *Proc. Natl. Acad. Sci. U. S. A.* **2008**, *105*, 17795−17800.

(12) Chawla, U.; Jiang, Y.; Zheng, W.; Kuang, L.; Perera, S. M.; Pitman, M. C.; Brown, M. F.; Liang, H. A Usual G-Protein-Coupled Receptor in Unusual Membranes. *Angew. Chem., Int. Ed.* **2016**, *55*, 588−592.

(13) Smith, S. O. Structure and Activation of the Visual Pigment Rhodopsin. *Annu. Rev. Biophys.* **2010**, *39*, 309−328.

(14) Palczewski, K. G. Protein−Coupled Receptor Rhodopsin. *Annu. Rev. Biochem.* **2006**, *75*, 743−767.

(15) Li, J.; Edwards, P. C.; Burghammer, M.; Villa, C.; Schertler, G. F. X. Structure of Bovine Rhodopsin in a Trigonal Crystal Form. *J. Mol. Biol.* **2004**, *343*, 1409−1438.

(16) Okada, T.; Ernst, O. P.; Palczewski, K.; Hofmann, K. P. Activation of Rhodopsin: New Insights from Structural and Biochemical Studies. *Trends Biochem. Sci.* **2001**, *26*, 318−324.

(17) Standfuss, J.; Edwards, P. C.; D'Antona, A.; Fransen, M.; Xie, G.; Oprian, D. D.; Schertler, G. F. X. The Structural Basis of Agonist-Induced Activation in Constitutively Active Rhodopsin. *Nature* **2011**, *471*, 656−660.

(18) Altenbach, C.; Kusnetzow, A. K.; Ernst, O. P.; Hofmann, K. P.; Hubbell, W. L. High-Resolution Distance Mapping in Rhodopsin Reveals the Pattern of Helix Movement Due to Activation. *Proc. Natl. Acad. Sci. U. S. A.* **2008**, *105*, 7439−7444.

(19) Mamontov, E.; Chu, X.-Q. Water-Protein Dynamic Coupling and New Opportunities for Probing it at Low to Physiological Temperatures in Aqueous Solutions. *Phys. Chem. Chem. Phys.* **2012**, *14*, 11573−11588.

(20) Bhowmik, D.; Shrestha, U.; Perera, S. M. d. c.; Chawla, U.; Mamontov, E.; Brown, M. F.; Chu, X.-Q. Rhodopsin Photoactivation Dynamics Revealed by Quasi-Elastic Neutron Scattering. *Biophys. J.* **2015**, *108*, 61a.

(21) Frauenfelder, H.; Sligar, S. G.; Wolynes, P. G. The Energy Landscapes and Motions of Proteins. *Science* **1991**, *254*, 1598−1603.

(22) Henzler-Wildman, K. A.; Lei, M.; Thai, V.; Kerns, S. J.; Karplus, M.; Kern, D. A Hierarchy of Timescales in Protein Dynamics is Linked to Enzyme Catalysis. *Nature* **2007**, *450*, 913−916.

(23) Karplus, M.; Vitkup, D.; Ringe, D.; Petsko, G. A. Solvent Mobility and the Protein 'Glass' Transition. *Nat. Struct. Biol.* **2000**, *7*, 34−38.

(24) Chu, X.-Q.; Lagi, M.; Mamontov, E.; Fratini, E.; Baglioni, P.; Chen, S.-H. Experimental Evidence of Logarithmic Relaxation in Single-Particle Dynamics of Hydrated Protein Molecules. *Soft Matter* **2010**, *6*, 2623−2627.

(25) Hong, L.; Smolin, N.; Lindner, B.; Sokolov, A. P.; Smith, J. C. Three Classes of Motion in the Dynamic Neutron-Scattering Susceptibility of a Globular Protein. *Phys. Rev. Lett.* **2011**, *107*, 148102.

(26) Doster, W.; Cusack, S.; Petry, W. Dynamical Transition of Myoglobin Revealed by Inelastic Neutron Scattering. *Nature* **1989**, *337*, 754−756.

(27) Gabel, F. Protein Dynamics in Solution and Powder Measured by Incoherent Elastic Neutron Scattering: The Influence of Q-Range and Energy Resolution. *Eur. Biophys. J.* **2005**, *34*, 1−12.

(28) Zaccai, G. How Soft is a Protein? A Protein Dynamics Force Constant Measured by Neutron Scattering. *Science* **2000**, *288*, 1604−1607.

(29) Chu, X.-Q.; Gajapathy, M.; Weiss, K. L.; Mamontov, E.; Ng, J. D.; Coates, L. Dynamic Behavior of Oligomeric Inorganic Pyrophosphatase Explored by Quasielastic Neutron Scattering. *J. Phys. Chem. B* **2012**, *116*, 9917−9921.

(30) Ringe, D.; Petsko, G. A. The 'Glass Transition' in Protein Dynamics: What it is, Why it Occurs, and How to Exploit it. *Biophys. Chem.* **2003**, *105*, 667−680.

(31) Bhowmik, D.; Malikova, N.; Teixeira, J.; Mériguet, G.; Bernard, O.; Turq, P.; Häussler, W. Study of Tetrabutylammonium Bromide in Aqueous Solution by Neutron Scattering. *Eur. Phys. J.: Spec. Top.* **2012**, *213*, 303−312.

(32) Chu, X.-Q.; Mamontov, E.; O'Neill, H.; Zhang, Q. Apparent Decoupling of the Dynamics of a Protein from the Dynamics of Its Aqueous Solvent. *J. Phys. Chem. Lett.* **2012**, *3*, 380−385.

(33) Khodadadi, S.; Sokolov, A. P. Protein Dynamics: From Rattling in a Cage to Structural Relaxation. *Soft Matter* **2015**, *11*, 4984−4998.

(34) Bhowmik, D.; Pomposo, J. A.; Juranyi, F.; Garcia Sakai, V.; Zamponi, M.; Arbe, A.; Colmenero, J. Investigation of a Nanocomposite of 75 Wt % Poly(Methyl Methacrylate) Nanoparticles with 25 Wt % Poly(Ethylene Oxide) Linear Chains: A Quasielatic Neutron Scattering, Calorimetric, and Waxs Study. *Macromolecules* **2014**, *47*, 3005−3016.

(35) Bhowmik, D.; Pomposo, J. A.; Juranyi, F.; Garcia-Sakai, V.; Zamponi, M.; Su, Y.; Arbe, A.; Colmenero, J. Microscopic Dynamics in Nanocomposites of Poly(Ethylene Oxide) and Poly(Methyl Methacrylate) Soft Nanoparticles: A Quasi-Elastic Neutron Scattering Study. *Macromolecules* **2014**, *47*, 304−315.

(36) Bhowmik, D.; Malikova, N.; Mériguet, G.; Bernard, O.; Teixeira, J.; Turq, P. Aqueous Solutions of Tetraalkylammonium Halides: Ion Hydration, Dynamics and Ion-Ion Interactions in Light of Steric Effects. *Phys. Chem. Chem. Phys.* **2014**, *16*, 13447−57.

(37) Dhindsa, G. K.; Bhowmik, D.; Goswami, M.; O'Neill, H.; Mamontov, E.; Sumpter, B. G.; Hong, L.; Ganesh, P.; Chu, X.-Q. Enhanced Dynamics of Hydrated tRNA on Nanodiamond Surfaces: A Combined Neutron Scattering and MD Simulation Study. *J. Phys. Chem. B* **2016**, DOI: 10.1021/acs.jpcb.6b07511.

(38) Chathoth, S. M.; Mamontov, E.; Melnichenko, Y. B.; Zamponi, M. Diffusion and Adsorption of Methane Confined in Nano-Porous Carbon Aerogel: A Combined Quasi-Elastic and Small-Angle Neutron Scattering Study. *Microporous Mesoporous Mater.* **2010**, *132*, 148−153.

(39) Lagi, M.; Baglioni, P.; Chen, S.-H. Logarithmic Decay in Single-Particle Relaxation of Hydrated Lysozyme Powder. *Phys. Rev. Lett.* **2009**, *103*, 108102.

(40) Bhowmik, D.; Dhindsa, G. K.; Rusek, A. J.; Van Delinder, K.; Shrestha, U. R.; Ng, J. D.; Sharp, M.; Stingaciu, L. R.; Chu, X.-q. Probing the Domain Motions of an Oligomeric Protein from Deep-Sea Hyperthermophile by Neutron Spin Echo. *Biophys. J.* **2015**, *108*, 59a.

(41) Arbe, A.; Pomposo, J. A.; Asenjo-Sanz, I.; Bhowmik, D.; Ivanova, O.; Kohlbrecher, J.; Colmenero, J. Single Chain Dynamic Structure Factor of Linear Polymers in an All-Polymer Nano-Composite. *Macromolecules* **2016**, *49*, 2354−2364.

(42) Austin, R. H.; Beeson, K. W.; Eisenstein, L.; Frauenfelder, H.; Gunsalus, I. C. Dynamics of Ligand-Binding to Myoglobin. *Biochemistry* **1975**, *14*, 5355−5373.

(43) Onuchic, J. N.; Luthey-Schulten, Z.; Wolynes, P. G. Theory of Protein Folding: The Energy Landscape Perspective. *Annu. Rev. Phys. Chem.* **1997**, *48*, 545−600.

(44) Shrestha, U. R.; Bhowmik, D.; Copley, J. R. D.; Tyagi, M.; Leão, J. B.; Chu, X.-Q. Effects of Pressure on the Dynamics of an Oligomeric Protein from Deep-Sea Hyperthermophile. *Proc. Natl. Acad. Sci. U. S. A.* **2015**, *112*, 13886−13891.

(45) Angell, C. A. Formation of Glasses from Liquids and Biopolymers. *Science* **1995**, *267*, 1924−1935.

(46) Green, J. L.; Fan, J.; Angell, C. A. The Protein-Glass Analogy: Some Insights from Homopeptide Comparisons. *J. Phys. Chem.* **1994**, *98*, 13780−13790.

(47) Gotze, W.; Sjogren, L. Relaxation Processes in Supercooled Liquids. *Rep. Prog. Phys.* **1992**, *55*, 241.

(48) Chu, X.-Q.; Mamontov, E.; O'Neill, H.; Zhang, Q. Temperature Dependence of Logarithmic-Like Relaxational Dynamics of Hydrated tRNA. *J. Phys. Chem. Lett.* **2013**, *4*, 936−942.

(49) Götze, W.; Sperl, M. Logarithmic Relaxation in Glass-Forming Systems. *Phys. Rev. E: Stat. Phys., Plasmas, Fluids, Relat. Interdiscip. Top.* **2002**, *66*, 011405.

(50) Shrestha, U.; Bhowmik, D.; Perera, S. M. D. C.; Chawla, U.; Struts, A. V.; Graziano, V.; Qian, S.; Heller, W. T.; Brown, M. F.; Chu, X.-Q. Small Angle Neutron and X-Ray Scattering Reveal Conformational Differences in Detergents Affecting Rhodopsin Activation. *Biophys. J.* **2015**, *108*, 39a.

(51) Lill, M. A. Efficient Incorporation of Protein Flexibility and Dynamics into Molecular Docking Simulations. *Biochemistry* **2011**, *50*, 6157−6169.

(52) Struts, A. V.; Salgado, G. F. J.; Martínez-Mayorga, K.; Brown, M. F. Retinal Dynamics Underlie its Switch from Inverse Agonist to Agonist During Rhodopsin Activation. *Nat. Struct. Mol. Biol.* **2011**, *18*, 392−394.

(53) Frauenfelder, H.; Fenimore, P. W.; Chen, G.; McMahon, B. H. Protein Folding is Slaved to Solvent Motions. *Proc. Natl. Acad. Sci. U. S. A.* **2006**, *103*, 15469−15472.

(54) Chen, S. H.; Liu, L.; Fratini, E.; Baglioni, P.; Faraone, A.; Mamontov, E. Observation of Fragile-to-Strong Dynamic Crossover in Protein Hydration Water. *Proc. Natl. Acad. Sci. U. S. A.* **2006**, *103*, 9012−9016.

(55) Leioatts, N.; Mertz, B.; Martinez-Mayorga, K.; Romo, T. D.; Pitman, M. C.; Feller, S. E.; Grossfield, A.; Brown, M. F. Retinal Ligand Mobility Explains Internal Hydration and Reconciles Active Rhodopsin Structures. *Biochemistry* **2014**, *53*, 376−385.